


# Impact of Iron Tallate on the Kinetic Behavior of the Oxidation Process of Heavy Oils

Mohammed A. Khelkhal, Alexey A. Eskin, Sergey A. Sitnov, and Alexey V. Vakhin\*

Institute of Geology and Petroleum Technologies, Kazan Federal University, Kazan 420008, Russia

**ABSTRACT:** Oxidation of heavy and extra-heavy oils is recognized as a complicated process due to the heterogeneous nature of its reaction medium and the lack of knowledge concerning its reaction mechanisms. The next decade is likely to witness a considerable rise in the use of in situ combustion to extract heavy and extra-heavy oils. However, a major issue of the in situ combustion is the instability of the combustion front. For this reason, application of catalysts was viewed as a way to initiate the process early and stabilize the resultant combustion front. In this study, we have synthesized an efficient precursor of iron-containing catalyst, studied its effect on heavy-oil oxidation by estimating the heat-flow-rate changes occurring during the oxidation process as a function of heating at different rates using differential scanning calorimetry, and investigated its transformation throughout the oxidation process by estimating its mass loss with heating at the rate of  $10\text{ }^{\circ}\text{C min}^{-1}$  using thermogravimetric analysis. In addition, we studied the morphology and size of the final product of oxidation obtained at  $500\text{ }^{\circ}\text{C}$  using scanning electron microscopy. At the end of the study, we compared its effect to that of the previously studied manganese tallate on heavy-oil oxidation. The kinetic parameters of the processes have been obtained by means of applying Kissinger method (isoconversional principle). Interestingly, iron tallate has been found to decrease the activation energy of both low-temperature and high-temperature oxidation regions. In addition, the values of effective reaction rate constants of both regions (low-temperature oxidation and high-temperature oxidation) increased in the presence of iron tallate as well. Moreover, it has been suggested that the iron oxide nanoparticles formed in situ are responsible for the resulting catalytic effect.

## 1. INTRODUCTION

Fossil energy is a vital factor in increasing economy and for satisfying industrial demand. Nevertheless, sustaining it remains a hard task to achieve due to its limited reserves. Experts have always seen conventional oils as an important source for providing and satisfying the energy demand since their extraction and transportation are relatively uncomplicated. However, it is not yet known how long they could be available for future exploitation. Therefore, looking for new ways to maintain the energy sector has become a necessity. The next few years are likely to see a considerable rise in exploiting and developing other types of oils known as unconventional oils.<sup>1</sup> Among unconventional oils, heavy and extra-heavy oils are attracting widespread interest due to their potential amounts, according to experts.<sup>2</sup> High viscosity, high density, and high amount of metal and sulfur are common issues of heavy and extra-heavy oils, which make their exploitation difficult and may cause pollution.<sup>3,4</sup> Thus, developing new methods that are able to play a dual role of facilitating their exploitation and generating a positive impact on the surrounding is indeed an important task that should be taken into consideration.

Recent developments in the field of high-viscosity-oil exploitation have led to the adoption of different methods based on injecting chemicals, gases, and heat to enhance its recovery. This group of methods became known as enhanced oil recovery (EOR) methods.<sup>5,6</sup> The term ThEOR has been applied to the thermally enhanced oil recovery methods and has attracted increasing interest from the industry for exploitation of unconventional oils.<sup>7,8</sup> In general terms, ThEOR can be defined as a way to decrease the viscosity of heavy or extra-heavy oil by using heat that is either generated

inside the reservoir or transferred from the surface to the reservoir.<sup>9</sup> Among the aforementioned methods, in situ combustion has been always seen as a promising method for exploiting these types of oils.<sup>10</sup> It is based on injecting air into the reservoir; as a result, a part of the reservoir gets burned under the present temperature and pressure, resulting in a combustion front flowing throughout the reservoir.<sup>11</sup> During the in situ combustion, two main processes occur in different temperature regions, namely, low-temperature oxidation (LTO) and high-temperature oxidation (HTO).<sup>12</sup> In the low-temperature oxidation, the injected air reacts with oil and leads to oxygenated compounds (alcohols, peroxides, carbonyl compounds), while the high-temperature oxidation is believed to be the region where coke is oxidized into carbon oxide and water.<sup>13</sup>

The combustion front is considered to be a critical element in the hole process of the in situ combustion.<sup>14</sup> One of the main issues known about the combustion front is the lack of stability and an earlier breakthrough even in the early stages of the process.<sup>15</sup> Moreover, few pilot tests have been successfully applied since its first invention in the beginning of the last century.<sup>16–18</sup> To solve this problem, most studies have tended to focus on the application of transition-metal catalysts because they are widely used in petroleum industry, in addition to their particular electrical, physical, and chemical properties.<sup>19–21</sup> The catalysts used for enhancing heavy-oil recovery are generally classified as water soluble; oil soluble; amphiphilic;

Received: May 3, 2019

Revised: June 11, 2019

Published: July 1, 2019



Table 1. Physical Properties of Ashalcha Heavy Oil at 20 °C

viscosity, mPa s	density, g cm <sup>-3</sup>	API gravity	elemental content, %				SARA analysis, %			
			C	H	N	S	saturated	aromatic	resins	asphaltenes
11 811	0.97	13.8	82.09	10.12	0.63	2.65	26.2 ± 0.5	44.1 ± 0.6	26.3 ± 0.5	4.5 ± 0.3

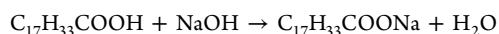
minerals; and zeolites, solid superacids, and dispersed nanoparticles.<sup>22–28</sup> Oil-soluble catalysts showed significant efficiency in different works. For example, in the work<sup>29</sup> of Ramirez-Garnica et al., organometallic precursors of iron-, nickel-, molybdenum-, and cobalt-containing catalysts were used in the combustion of Gulf-Mexican heavy oil using combustion tubes. The results highlighted an improvement in the characteristics of the in situ combustion in the presence of these catalysts compared to when they are absent when the combustion front flow was faster and the oil production was well enhanced. In addition, our previous studies<sup>30–32</sup> on the oxidation of Ashalcha heavy oil have demonstrated similar results in the presence of manganese acetylacetonates and manganese tallate in terms of enhancing the oxidation reactions occurring during the process of in situ combustion using thermal analysis.

When it comes to oil-soluble catalysts, three crucial factors should be taken into account: efficiency, positive impact on surrounding, and availability. It has been suggested that catalysts<sup>33–37</sup> based on tall oil possess these characteristics since they are environmentally friendly, cheap, and highly dispersive in oil media. Therefore, the use of metal tallate as a catalyst for the process of heavy-oil in situ combustion seems to be reliable. On the other hand, it is a common knowledge that iron is widely used in the catalysis and its application leads almost to better results.<sup>38</sup> Therefore, we believe that iron tallate may play an important role in the process of heavy-oil combustion. This paper is divided into three main sections. The first section studies the kinetic parameters of both LTO and HTO regions in the presence and absence of iron tallate. The second section highlights the morphology and structure of catalytic agents responsible for enhancing the oxidation process, and the last section compares the effects of iron tallates and manganese tallates obtained in previous works on heavy-oil oxidation process.

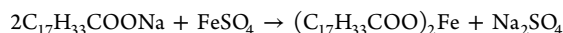
## 2. EXPERIMENTAL SECTION

**2.1. Materials.** The studied oil was kindly provided by Tatneft oil company from Ashalcha oilfield (Volga-Ural basin, Republic of Tatarstan, Russia) and is described in Table 1. Organic solvents (purity more than 99.5%) were purchased from Component Reactiv and used without additional purification. Inorganic salts and pure quartz sand fraction of 43–64 μm were obtained from Sigma-Aldrich.

**2.2. Sample Preparation.** Iron tallate was obtained according to a well-known method.<sup>37</sup> The molecular precursor was synthesized using distilled tall oil (DTO) as a ligand-forming agent. Iron carboxylate has been obtained by exchange reactions of inorganic metal salt with the sodium salt of DTO. The process of fatty acids saponification is described by the following equation



carboxylate interacts with the iron salt when heated as follows



DTO was loaded into a three-necked flask equipped with a thermometer and a stirrer, heated to 75–80 °C, and finally a stoichiometric amount of sodium hydroxide solution added for 1.5 h with continuous stirring. The temperature of the reaction was maintained within 75–80 °C. After adding the total amount of alkali,

the reaction was kept at the same temperature for 1.0–1.5 h to ensure the complete interaction of alkali with the DTO carboxyl groups. Then, at 75–80 °C, a solution of iron salt was added to the reaction system. The obtained iron tallate was dark brown with high viscosity.

To investigate the effect of catalyst on the oxidation process, a heavy oil (10.0 wt %) with pure quartz sand fraction of 43–64 μm (90.0 wt %) was mixed for the noncatalytic process. For the catalytic process, 2 wt % of iron tallate was present in the initial sample of the oil.

**2.3. Thermal Analysis.** Differential scanning calorimetry (DSC) and thermogravimetric analysis (TGA) experiments were applied by means of STA 449 F1 Jupiter (Netzsch) thermoanalyzer in the temperature range of 30–600 °C. The experiments were conducted at linear heating rates of 5, 10, 15, and 20 °C min<sup>-1</sup> under 50 mL min<sup>-1</sup> airflow. Data management was performed by Proteus Analysis v5.2.1, NETZSCH Peak Separation (version 2010.09) and NETZSCH Thermokinetics 3.1 (version 06.08.2014) program packages.

Generally speaking, oil oxidation process is believed to be a complex, poorly studied process including different complex reactions in heterogeneous media combined with diffusion processes. For this reason, its kinetic study presents a hard task and usually its reaction rate is expressed by two main parameters: conversion degree  $\alpha$  and oxygen partial pressure<sup>11</sup> as follows

$$\frac{d\alpha}{dt} = k(T)P_{O_2}^a(1 - \alpha)^b \quad (1)$$

where  $\alpha$  could be calculated via the DSC peaks fractional areas,  $b$  is the reaction order, and  $P_{O_2}$  is the oxygen partial pressure.

The rate constant  $k(T)$  obeys the Arrhenius law (eq 2)

$$k(T) = A e^{-E/RT} \quad (2)$$

Initial studies<sup>12,39</sup> have proposed that the oil-oxidation reaction order tends to be unity ( $b = 1$ ) relative to oil concentration and oxygen partial pressure. Moreover, the small size of the studied samples in a large furnace at a high airflow during DSC experiments suggests that the oxygen partial pressure is constant throughout the experiment, which gives the following equation

$$\frac{d\alpha}{dt} = k_{\text{eff}}(1 - \alpha) \quad (3)$$

where  $k_{\text{eff}} = kP_{O_2}$ .

**2.4. Kinetic Analysis.** It was decided that the best method to use for calculating the kinetic parameters of the oxidation process in this study is Kissinger's method.<sup>40</sup> It was preferred over other isoconversional methods because it eliminates the choice of baseline and peak profiles, i.e., it provides a simple and direct approach to calculate the kinetic parameters via peak temperatures at different heating rates. Its equation is presented as follows

$$\ln\left(\frac{\beta}{T_p^2}\right) = -\frac{E}{R} \times \frac{1}{T_p} + \ln(Af'(\alpha)) \quad (4)$$

where  $\beta$  and  $T_p$  are the heating rate and the peak temperature, respectively.

## 3. RESULTS AND DISCUSSION

We chose differential scanning calorimetry (DSC) and thermogravimetric analysis (TGA) in our study because they are one of the most rapid, feasible, and economic ways to estimate the kinetic parameters<sup>41,42</sup> of heavy-oil oxidation process in the presence and absence of iron tallate. In addition,

we applied scanning electron microscopy (SEM) on the product of thermal decomposition of iron tallowate at 500 °C. This method has many interesting characteristics, allowing to obtain the morphology and the size of the studied substances.

**3.1. Kinetic Calculations.** DSC was used to compare the oxidation behavior of heavy-oil oxidation in the absence of iron tallowate to its oxidation in its presence. Figure 1 shows the DSC

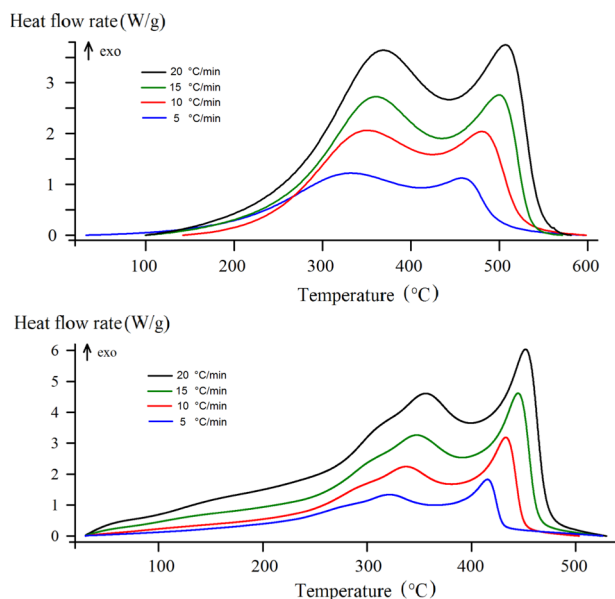


**Figure 1.** DSC curves for noncatalytic (top) and catalytic (bottom) oxidations of Ashalcha heavy oil.

curves for both processes. There were slight differences between catalytic oxidation and noncatalytic oxidation in the low-temperature oxidation (LTO) region with regard to peak temperatures shifts at different heating rates. However, a strong evidence of iron tallowate effect was found in the high-temperature oxidation (HTO) region where peak temperature shifts at different heating rates were considerable. Table 2

**Table 2.** DSC Reaction Intervals and Peak Temperatures

sample	$\beta$ , °C min <sup>-1</sup>	non catalytic		catalytic	
		interval, °C	$T_p$ , °C	interval, °C	$T_p$ , °C
LTO	5	234–369	324	260–350	321
	10	270–379	343	270–375	338
	15	340–398	354	335–390	348
	20	349–409	363	340–405	356
HTO	5	397–486	472	410–500	415
	10	459–510	493	418–440	433
	15	481–527	506	425–475	445
	20	494–537	515	440–480	452

provides the reaction intervals of LTO and HTO in both catalytic and noncatalytic processes in detail, and Figure 2 illustrates differences between the peak temperatures ( $\Delta T_p$ ) of noncatalytic and catalytic oxidations of heavy oils in the low- and high-temperature oxidation regions at different heating rates.

As anticipated, Kissinger's plots for the oxidation of heavy oil in the presence and absence of iron tallowate in both LTO and HTO regions (Figure 3) confirm the efficiency of iron tallowate in the process. However, the kinetic parameters grouped in

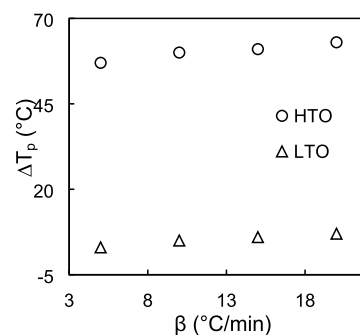


**Figure 2.** Differences between the peak temperatures ( $\Delta T_p$ ) of noncatalytic and catalytic oxidations of Ashalcha heavy oil in the low- and high-temperature regions at different heating rates.

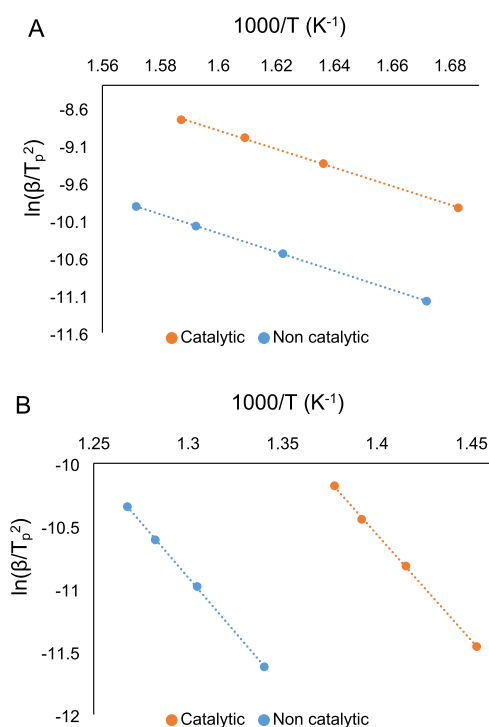


**Figure 3.** Kissinger's plots for the catalytic and noncatalytic oxidations of Ashalcha heavy oil ((A) is LTO, (B) is HTO).

Table 3 reveal some inconsistency concerning the energy of activation and pre-exponential factor. The activation energy decreases slightly in the presence of iron tallowate, which increases the reaction rate constant according to eq 2. The same situation is marked for the pre-exponential factor, which increases in the presence of iron tallowate and hence increases the reaction rate constant as well. For this reason, these findings need to be interpreted with caution.

Further calculations have been performed to find out the reaction rate constant of each process in both LTO and HTO regions. Figure 4 illustrates the difference between effective reaction rate constants of both LTO and HTO regions in catalytic and noncatalytic oxidations. The results are in complete agreement with our aforementioned hypothesis concerning DSC curves, Kissinger's plots, and the obtained kinetic parameters, where we see higher values for the reaction rate constant in the catalytic oxidation compared to the noncatalytic one in the high-temperature oxidation region, whereas this difference is slight in the LTO region. This can be

Table 3. Kinetic Parameters of the Oxidation Processes

	noncatalytic		catalytic	
	LTO	HTO	LTO	HTO
$E_a$ , kJ mol <sup>-1</sup>	104.6 ± 1.8	145.8 ± 8.3	102.9 ± 1.7	140.3 ± 8.4
log <sub>10</sub> A, A in min <sup>-1</sup>	9.8	11.9	10.9	13.1

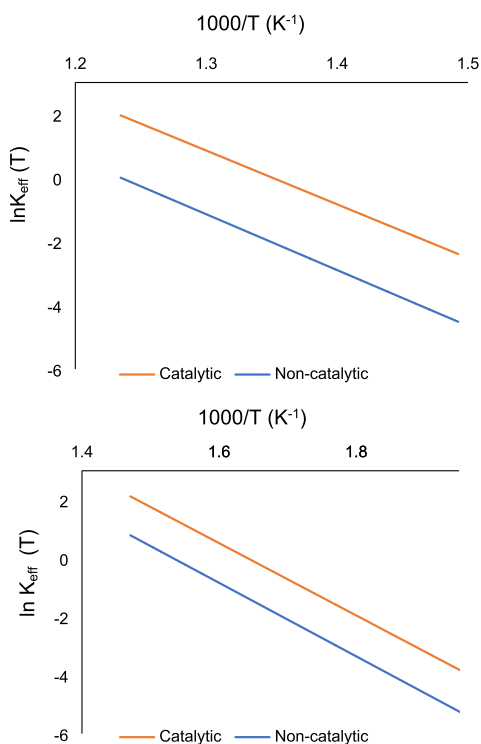


Figure 4. Variation of effective reaction rate constants with temperature in catalytic and noncatalytic oxidations (top is for LTO, bottom is for HTO).

explained by the speeding up of fuel deposition since iron tallate decreases the activation energy of LTO, and therefore the early combustion front appears compared to that in the noncatalytic oxidation as mentioned by Moore et al. in their work.<sup>43</sup> As a result of the early formation of the combustion front, HTO reactions are expected to occur earlier as well compared to the noncatalytic HTO reactions.

**3.2. Catalyst Characterization.** The second part in our current investigation reveals the agent responsible for the high efficiency of the catalyst in the high-temperature oxidation region. Therefore, we applied thermogravimetric analysis (TGA) on a sample of iron tallate at a heating rate of 10 °C min<sup>-1</sup> with a temperature program of 30–600 °C to describe the decomposition of iron tallate with temperature. As seen from Figure 5, the iron tallate decomposes at three main points at 278, 339, and 425–440 °C. We believe that at 278 °C, the organic part of iron tallate (fatty acids) starts decomposing and iron(II) oxide is formed. At 339 °C, we suggest that it is the point where most of the fatty acids decompose and Fe<sub>3</sub>O<sub>4</sub> is formed. In the last stage (425–440 °C), which is the region of high-temperature oxidation, we assume the formation of iron(III) oxide (Fe<sub>2</sub>O<sub>3</sub>) and the catalysis of the high-temperature oxidation region. Finally, we used scanning electron microscopy on a sample of iron tallate already heated under air atmosphere at 500 °C for 4 h. Figure 6 shows SEM

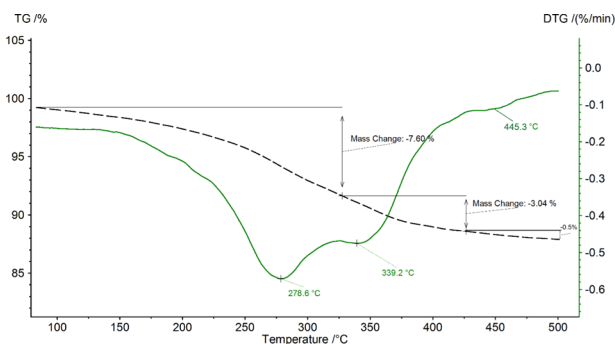


Figure 5. TG and DTG curves of the decomposition of iron tallate.

image of the obtained product. The result highlights iron oxide (Fe<sub>2</sub>O<sub>3</sub>) nanoparticles with an average size of 20 ± 5 nm.

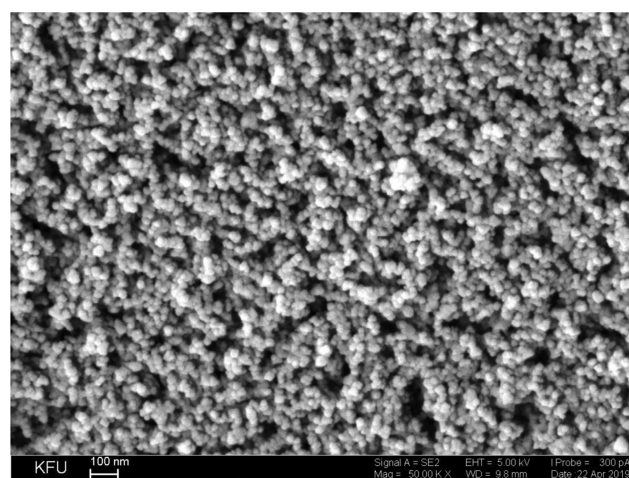
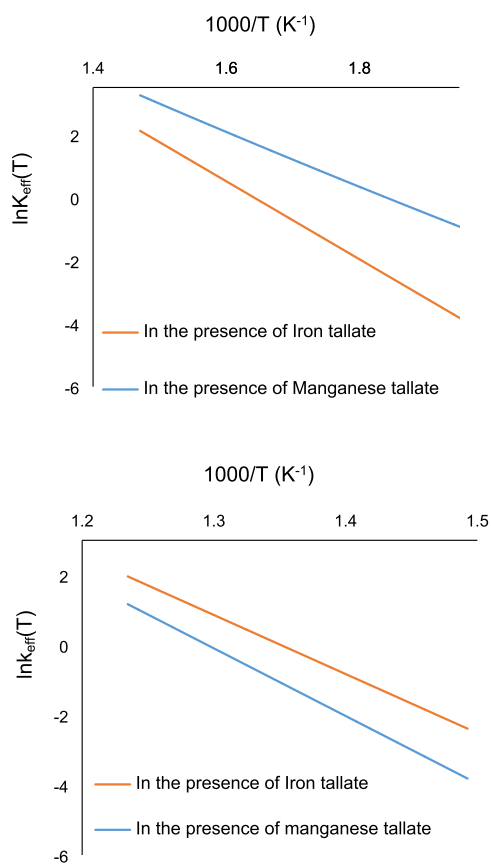


Figure 6. SEM image of the obtained Fe<sub>2</sub>O<sub>3</sub> nanoparticles from the decomposition of iron tallate at 500 °C.

In summary, the mechanism of the catalyst precursor during thermal decomposition could be explained by the interaction of metals with oxygen to form iron oxide nanoparticles as mentioned above. Iron oxide is usually used as a catalyst to break carbon–heteroatom bonds. Since the C–S bonds are weak, they can be broken easily using iron oxide and therefore lead to a decrease in the molecular weight of asphaltenes, which means a decrease in oil viscosity.

**3.3. Comparing Iron and Manganese Tallates Effect on Heavy-Oil Oxidation.** The obtained results in this study are consistent with the previous results using manganese tallates<sup>30</sup> in terms of decreasing activation energy of heavy-oil oxidation in porous media. However, the values of effective reaction rate constants were higher in the presence of manganese tallate compared to those obtained in the presence of iron tallate in the low-temperature oxidation region (Figure 7, bottom), which indicates the earlier initiation of combustion front in the presence of manganese tallate compared to that in the presence of iron tallate. In contrast, we found much higher



**Figure 7.** Variation of effective reaction rate constants with temperature in the presence of iron and manganese tallates (top is for LTO, bottom is for HTO).

values of effective reaction rate constants of the heavy-oil oxidation process in the presence of iron tallates than those found in the presence of manganese tallate in the high-temperature oxidation region (Figure 7, bottom). As argued by Niu et al.,<sup>44</sup> the LTO reactions can be affected by the following parameters: oxygen pressure, water saturation, and formation rocks. In our study, we considered the aforementioned parameters as constant; therefore, the only parameter remaining to be evaluated in the process was the effect of catalyst. The LTO reactions play an important role in forming fuel, which is the origin of the combustion front in the reservoir.<sup>45</sup> However, the slight difference in the values of effective reaction rate constants in the presence of iron tallate and manganese tallate expresses that the quantity of fuel deposition should be almost the same. For this reason, we focused more on the effect of catalysts on the high-temperature oxidation process since it is associated with the end of the process. Therefore, iron tallate could be more effective than manganese tallate in the in situ combustion of heavy oils.

#### 4. CONCLUSIONS

In sum, this paper presented the effect of iron tallate on the process of heavy-oil oxidation in porous media. We have synthesized an efficient precursor of iron-containing catalyst, studied its effect on heavy-oil oxidation using DSC, investigated its transformation throughout the oxidation process using TGA, and studied its morphology and size at the end of the process using SEM. In addition, we compared its effect to that of the previously studied manganese tallate on

heavy-oil oxidation. Taken together, the obtained results would seem to suggest that iron tallate is an efficient catalyst for upgrading heavy oil by means of in situ combustion, where it decreased the activation energy in both the low-temperature oxidation and high-temperature oxidation regions. Interestingly, iron tallate has been found to increase the values of effective reaction rate constants in the low-temperature oxidation and high-temperature oxidation regions, which is considered a key for the earlier initiation and promotion of the combustion front. Our study provides encouragement to use tallates as an environmentally friendly base for catalysts of oil oxidation processes. Our work clearly has some limitations. Despite this, we believe that it could be the starting point to achieve more success in the application of in situ combustion process. In addition, the present findings might have important implications for solving problem of early breakdown of the combustion front during the oxidation of heavy oils in porous media. To further our research, we are planning to synthesize iron oxide nanoparticles with special properties and investigate their effect on the oxidation of Ashalcha heavy oil. We hope that future tests will confirm our findings.

#### ■ AUTHOR INFORMATION

##### Corresponding Author

\*E-mail: [vahin-a\\_v@mail.ru](mailto:vahin-a_v@mail.ru).

##### ORCID

Alexey V. Vakhin: 0000-0002-5168-7063

##### Notes

The authors declare no competing financial interest.

#### ■ ACKNOWLEDGMENTS

The work is performed according to the Russian Government Program of Competitive Growth of Kazan Federal University.

#### ■ REFERENCES

- (1) Vilamová, Š.; Piecha, M.; Pavelek, Z. Unconventional Oil Resources Exploitation: A Review. *Acta Montan. Slovaca* **2016**, *21*, 247–257.
- (2) Cander, H. In What Is Unconventional Resources, Proceedings of the AAPG Annual Convention and Exhibition, Long Beach, CA, 2012; pp 22–25.
- (3) Hyne, J. B.; Clark, P. D.; Clarke, R. A.; Koo, J.; Greidanus, J. W. Aquathermolysis of Heavy Oils. *Rev. Tec. INTEVEP* **1982**, *2*, 87–94.
- (4) Oknina, N.; Kadiev, K.; Kadieva, M.; Maksimov, A.; Batov, A.; Dandaev, A. Physico-Chemical Properties of Oil Sludges from Reservoirs. *Biosci., Biotechnol. Res. Asia* **2015**, *12*, 497–505.
- (5) Kök, M. V.; Varfolomeev, M. A.; Nurgaliev, D. K. Application of Different EOR Techniques for the Energy and Recovery of Ashal'cha Oil Field. *Energy Sources, Part A* **2018**, *40*, 645–653.
- (6) Koottungal, L. 2008 Worldwide EOR Survey. *Oil Gas J.* **2008**, *106*, 47.
- (7) Khakimova, L.; Bondarenko, T.; Cheremisin, A.; Myasnikov, A.; Varfolomeev, M. High Pressure Air Injection Kinetic Model for Bazhenov Shale Formation Based on a Set of Oxidation Studies. *J. Pet. Sci. Eng.* **2019**, *172*, 1120–1132.
- (8) Stahl, C. R.; Gibson, M. A.; Knudsen, C. W. Thermally-Enhanced Oil Recovery Method and Apparatus. U.S. Patent US4694907; Sept 22, 1987, p 13.
- (9) Boberg, T. C. *Thermal Methods of Oil Recovery*; U.S. Department of Energy, 1988.
- (10) Castanier, L. M.; Brigham, W. E. In-Situ Combustion. In *Society of Petroleum Engineers Handbook*; Society of Petroleum Engineers, 2004.
- (11) Sarathi, P. S. *In-Situ Combustion Handbook--Principles and Practices*; National Petroleum Technology Office: Tulsa, OK, 1999.

- (12) Fassihi, M. R.; Brigham, W. E.; Ramey, H. J., Jr. Reaction Kinetics of In-Situ Combustion: Part 2—Modeling. *Soc. Pet. Eng. J.* **1984**, *24*, 399–407.
- (13) Sarathi, P. *In-Situ Combustion Handbook—Principles and Practices*; National Petroleum Technology Office: Tulsa, OK, 1999.
- (14) Bagci, S. Estimation of Combustion Zone Thickness during in Situ Combustion Processes. *Energy Fuels* **1998**, *12*, 1153–1160.
- (15) Shen, C. In Limitations and Potentials of In-Situ Combustion Processes for Heavy Oil Reservoirs, Canadian International Petroleum Conference; Petroleum Society of Canada, 2002; pp 1–14.
- (16) Panait-Patica, A.; Serban, D.; Ilie, N.; Pavel, L.; Barsan, N. In *Suplacu de Barcau Field—a Case History of a Successful In-Situ Combustion Exploitation*, SPE Europec/EAGE Annual Conference and Exhibition, Society of Petroleum Engineers, 2006; p 10.
- (17) Moss, J. T.; White, P. D. In *In Situ Combustion Process - Results of a Five-Well Field Experiment in Southern Oklahoma*, Society of Petroleum Engineers, 1959.
- (18) Machedon, V.; Popescu, T.; Paduraru, R. In *Romania-30 Years of Experience in in Situ Combustion*, BDM Oklahoma, Inc.; National Institute for Petroleum and Energy Research, Bartlesville, OK, 1995.
- (19) Kumar, S.; Srivastava, M. Catalyzing Mesophase Formation by Transition Metals. *J. Anal. Appl. Pyrolysis* **2015**, *112*, 192–200.
- (20) Hart, A.; Greaves, M.; Wood, J. A Comparative Study of Fixed-Bed and Dispersed Catalytic Upgrading of Heavy Crude Oil Using-CAPRI. *Chem. Eng. J.* **2015**, *282*, 213–223.
- (21) Hamed Shokrlu, Y.; Babadagli, T. In-Situ Upgrading of Heavy Oil/Bitumen During Steam Injection by Use of Metal Nanoparticles: A Study on In-Situ Catalysis and Catalyst Transportation. *SPE Reservoir Eval. Eng.* **2013**, *16*, 333–344.
- (22) Boukherissa, M.; Mutelet, F.; Modarressi, A.; Dicko, A.; Dafri, D.; Rogalski, M. Ionic Liquids as Dispersants of Petroleum Asphaltenes. *Energy Fuels* **2009**, *23*, 2557–2564.
- (23) Li, Y.-B.; Gao, H.; Pu, W.-F.; Li, L.; Chen, Y.; Bai, B. Study of the Catalytic Effect of Copper Oxide on the Low-Temperature Oxidation of Tahe Ultra-Heavy Oil. *J. Therm. Anal. Calorim.* **2019**, *135*, 3353–3362.
- (24) Kniazeva, M.; Maximov, A. Effect of Additives on the Activity of Nickel–Tungsten Sulfide Hydroconversion Catalysts Prepared In Situ from Oil-Soluble Precursors. *Catalysts* **2018**, *8*, 644.
- (25) Kok, M. V. The Thermal Characterization of Crude Oils in a Limestone Matrix of Different Particle Size. *Energy Sources, Part A* **2014**, *36*, 923–928.
- (26) Guo, K.; Li, H.; Yu, Z. In-Situ Heavy and Extra-Heavy Oil Recovery: A Review. *Fuel* **2016**, *185*, 886–902.
- (27) Mukhamatdinov, I. I.; Salih, I. S.; Vakhin, A. V. Changes in the Subfractional Composition of Heavy Oil Asphaltenes under Aquathermolysis with Oil-Soluble CO-Based Catalyst. *Pet. Sci. Technol.* **2019**, *37*, 1589–1595.
- (28) Salih, I. S. S.; Mukhamatdinov, I. I.; Vahin, A. V.; Garifullina, E. I. In *Fractional composition of heavy oil asphaltenes of volga-ural petroleum province*, International Multidisciplinary Scientific Geo-Conference Surveying Geology and Mining Ecology Management, SGEM, 2017; Vol. 17, 1.5; pp 485–491.
- (29) Nares, R.; Schacht-Hernandez, P.; Ramirez-Garnica, M. A.; Cabrera-Reyes, M. del C. Increase Heavy-Oil Production in Combustion Tube Experiments Through the Use of Catalyst. In *Combustion*; Society of Petroleum Engineers, 2007; p 10.
- (30) Khelkhal, M. A.; Eskin, A. A.; Sharifullin, A. V.; Vakhin, A. V. Differential Scanning Calorimetric Study of Heavy Oil Catalytic Oxidation in the Presence of Manganese Tallates. *J. Pet. Sci. Technol.* **2019**, 1194–1200.
- (31) Galukhin, A.; Khelkhal, M. A.; Gerasimov, A.; Biktagirov, T.; Gafurov, M.; Rodionov, A.; Orlinskii, S. Mn-Catalyzed Oxidation of Heavy Oil in Porous Media: Kinetics and Some Aspects of the Mechanism. *Energy Fuels* **2016**, *30*, 7731–7737.
- (32) Galukhin, A. V.; Nosov, R.; Eskin, A.; Khelkhal, M. A.; Osin, Y. Manganese Oxides Nanoparticles Immobilized on Silica Nanospheres as a Highly Efficient Catalyst for Heavy Oil Oxidation. *Ind. Eng. Chem. Res.* **2019**, 8990.
- (33) Vakhin, A. V.; Aliev, F. A.; Kudryashov, S. I.; Afanasiev, I. S.; Petrashov, O. V.; Sitnov, S. A.; Mukhamatdinov, I. I.; Varfolomeev, M. A.; Nurgaliev, D. K. Aquathermolysis of Heavy Oil in Reservoir Conditions with the Use of Oil-Soluble Catalysts: Part I—Changes in Composition of Saturated Hydrocarbons. *J. Pet. Sci. Technol.* **2018**, *36*, 1829–1836.
- (34) Sitnov, S. A.; Mukhamatdinov, I. I.; Vakhin, A. V.; Ivanova, A. G.; Voronina, E. V. Composition of Aquathermolysis Catalysts Forming in Situ from Oil-Soluble Catalyst Precursor Mixtures. *J. Pet. Sci. Eng.* **2018**, *169*, 44–50.
- (35) Mikhailova, A. N.; Kayukova, G. P.; Kosachev, I. P.; Vandyukova, I. I.; Vakhin, A. V.; Batalin, G. A. The Influence of Transition Metals—Fe, Co, Cu on Transformation of Organic Matters from Domanic Rocks in Hydrothermal Catalytic System. *J. Pet. Sci. Technol.* **2018**, *36*, 1382–1388.
- (36) Kayukova, G. P.; Mikhailova, A. N.; Khasanova, N. M.; Morozov, V. P.; Vakhin, A. V.; Nazimov, N. A.; Sotnikov, O. S.; Khisamov, R. S. Influence of Hydrothermal and Pyrolysis Processes on the Transformation of Organic Matter of Dense Low-Permeability Rocks from Domanic Formations of the Romashkino Oil Field. *Geofluids* **2018**, *2018*, 1–14.
- (37) Feoktistov, D. A.; Kayukova, G. P.; Vakhin, A. V.; Sitnov, S. A. Catalytic Aquathermolysis of High-Viscosity Oil Using Iron, Cobalt, and Copper Tallates. *Chem. Technol. Fuels Oils* **2018**, *53*, 905–912.
- (38) Ovalles, C.; Filgueiras, E.; Morales, A.; Scott, C. E.; Gonzalez-Gimenez, F.; Pierre Embaid, B. Use of a Dispersed Iron Catalyst for Upgrading Extra-Heavy Crude Oil Using Methane as Source of Hydrogen. *Fuel* **2003**, *82*, 887–892.
- (39) Bousaid, I. S.; Ramey, H. J., Jr. Oxidation of Crude Oil in Porous Media. *Soc. Pet. Eng. J.* **1968**, *8*, 137–148.
- (40) Kissinger, H. E. Variation of Peak Temperature with Heating Rate in Differential Thermal Analysis. *J. Res. Natl. Bur. Stand.* **1956**, *57*, 217–221.
- (41) Kok, M. V.; Gundogar, A. S. DSC Study on Combustion and Pyrolysis Behaviors of Turkish Crude Oils. *Fuel Process. Technol.* **2013**, *116*, 110–115.
- (42) Varfolomeev, M.; Rakipov, I.; Isakov, D.; Nurgaliev, D.; Kok, M. Characterization and Kinetics of Siberian and Tatarstan Regions Crude Oils Using Differential Scanning Calorimetry. *J. Pet. Sci. Technol.* **2015**, 865.
- (43) Moore, R. G.; Lareshen, C. J.; Belgrave, J. D. M.; Ursenbach, M. G.; Mehta, S. A. R. In Situ Combustion in Canadian Heavy Oil Reservoirs. *Fuel* **1995**, *74*, 1169–1175.
- (44) Niu, B.; Ren, S.; Liu, Y.; Wang, D.; Tang, L.; Chen, B. Low-Temperature Oxidation of Oil Components in an Air Injection Process for Improved Oil Recovery. *Energy Fuels* **2011**, *25*, 4299–4304.
- (45) Cinar, M.; Castanier, L. M.; Kovscek, A. R. Isoconversional Kinetic Analysis of the Combustion of Heavy Hydrocarbons. *Energy Fuels* **2009**, *23*, 4003–4015.